

See discussions, stats, and author profiles for this publication at: <https://www.researchgate.net/publication/271520739>

Comparative study of autonomous path-following vehicle control via model predictive control and linear quadratic control

Article in Proceedings of the Institution of Mechanical Engineers Part D Journal of Automobile Engineering · January 2015

DOI: 10.1177/0954407014566031

CITATIONS

33

READS

1,161

2 authors, including:



Fitri Yakub

Universiti Teknologi Malaysia

84 PUBLICATIONS 254 CITATIONS

[SEE PROFILE](#)

Some of the authors of this publication are also working on these related projects:



Rollover mitigation controller design of heavy vehicle under typhoon scenario [View project](#)



stability of unmanned ground sport utility vehicles [View project](#)

Comparative study of autonomous path-following vehicle control via model predictive control and linear quadratic control

Fitri Yakub^{1,2} and Yasuchika Mori¹

Abstract

This paper describes a comparative study of steering and yaw moment control manoeuvres in the model predictive control and linear quadratic control approaches for path-following control of an autonomous vehicle. We present the effectiveness of the model predictive control and linear quadratic control approaches for stability control of the vehicle's lateral position and yaw angle for different control manoeuvres: two-wheel steering, four-wheel steering and direct yaw moment control. We then propose model predictive control with a feedforward controller to minimize the tracking errors of the lateral position and the yaw angle in an active front steering manoeuvre, and these are compared with the results from linear quadratic control that has a feedforward controller. Model predictive control is designed on the basis of the simple yaw–lateral motions of a single-track vehicle with a linear tyre model (i.e. a bicycle model), which is an approximation of the more realistic model of a vehicle with double-track yaw–roll motion with a non-linear tyre model (i.e. the Pacejka model). The linear quadratic controller is designed on the basis of the same approach as adopted for the model predictive controller to achieve a fair comparison. On the basis of a given trajectory, we simulate the manoeuvre of the vehicle at a low speed, a middle speed and a high speed because load transfer effects will influence the roll dynamics especially at a high speed. We also perform simulations on low-road-friction surfaces in a double-lane-change scenario with the aim of following the desired trajectory as closely as possible while maintaining the vehicle stability. The simulation results show that model predictive control through two-wheel steering and four-wheel steering with direct yaw moment control performed better in terms of trajectory tracking at a high forward speed and low road surface variation. The proposed model predictive control with a feedforward controller is shown to be effective in minimizing the trajectory tracking errors. For all control manoeuvres, model predictive control gives a better tracking performance than linear quadratic control does. In addition, when the roll dynamics are considered, model predictive control significantly improves the vehicle stability and the trajectory along the desired path.

Keywords

Autonomous vehicle, model predictive control, linear quadratic control, path-following control, feedforward controller, manoeuvre control

Date received: 8 April 2014; accepted: 4 December 2014

Introduction

One of the most popular optimal control techniques which is widely employed for controlling constrained linear or non-linear systems is the model predictive control (MPC) technique. MPC uses a mathematical dynamic process model to predict a future value and to optimize the process control performance.^{1, 2} The MPC model is easy to use at different levels of the process control structure and offers attractive solutions for regulation and tracking problems³ while guaranteeing stability.⁴ On the other hand, linear quadratic control

(LQC), which is also based on a quadratic cost function, is widely implemented for process control⁵ and

¹Graduate School of System Design, Tokyo Metropolitan University, Tokyo, Japan

²Malaysia-Japan International Institute of Technology, Universiti Teknologi Malaysia, Kuala Lumpur, Malaysia

Corresponding author:

Fitri Yakub, Graduate School of System Design, Tokyo Metropolitan University, Graduate School of System Design, 6-6 Asahigaoka, Tokyo, Japan.
 Email: mfitri.kl@utm.my

motion control.⁶ LQC's main advantage is that the optimal input signal can be obtained from the full state feedback, whereas optimization of MPC is implemented in closed-loop systems. However, LQC has limitations in systems where it is necessary to consider actuator limitations, e.g. it is difficult to restrict the manipulated variable or the controlled variable.⁷ Because of its advantages, MPC has been implemented in automotive applications covering a wide range of advanced control systems, such as various active safety and driver assistance systems,^{8, 9} vehicle dynamics systems,^{10, 11} driver modelling systems,^{12, 13} integrated chassis control systems^{14, 15} and other related topics in vehicle control. At present, the most important topics for researchers and automotive manufacturers are those related to the use of active safety systems such as active steering,¹⁶ active traction,¹⁷ active braking¹⁸ and active differentials¹⁹ or suspension²⁰ to coordinate and improve the vehicle handling, the stability and the ride comfort while avoiding collisions. In addition, there is currently much interest in the use of autonomous vehicles or robots for military purposes, further increasing the relevance of advanced automotive control.²¹

An autonomous or driverless car is a vehicle capable of fulfilling human transportation needs and of sensing its environment with high-end technology such as radars, global positioning systems and computer vision with onboard cameras. Advanced control systems in autonomous vehicles interpret sensory information to identify obstacles and appropriate navigation paths, as well as relevant signage. Descriptions of the best comparative study on predictive control strategies for autonomous guidance vehicles have been given by Park et al.²² and Falcone et al.,²³ where a non-linear vehicle dynamics model is used for controller design by active front steering in a double-lane-change scenario.

There have been many studies of different control manoeuvres, such as two-wheel steering (2WS), which uses front or rear steering,^{24, 25} four-wheel steering (4WS), which uses front and rear steering,^{26, 27} and direct yaw moment control (DYC), which uses driving or braking forces^{28–30} with different control strategies and purposes. Recent papers have focused on the lateral and yaw dynamics models, neglecting the roll dynamic model. By including the roll dynamics in the system, we can evaluate the effectiveness of controllers, especially under high-speed conditions. Here, it should be emphasized that we assume a given desired trajectory based on the work by Borrelli et al.³¹ and we assume that no disturbances or cross-wind will affect the system.

In this paper, we extend the concept of MPC to apply it to the autonomous vehicle manoeuvring problem where trajectory optimization is solved at each time step. From the known trajectory, we simulate motion of the vehicle at a low forward speed (10 m/s), a middle forward speed (20 m/s) and a high forward speed (25 m/s) on a low-friction surface (a wet earth road), following the trajectory as closely as possible in a double-

lane-change scenario while maintaining the stability of the vehicle. The control inputs for the system depend on the vehicle manoeuvres, namely a front steering angle for 2WS, front and rear steering angles for 4WS and front and rear driving or braking forces for DYC, while the control outputs are the yaw angle, the yaw rate and the lateral position of the vehicle, where we emphasize more the tracking of the lateral position. We compare the performance of the eight-degrees-of-freedom (8DoF) vehicle model for two different controllers: MPC and LQC based on a simple yaw-lateral two-degrees-of-freedom (2DoF) bicycle model without roll dynamics. Moreover, we evaluate and compare the values of the effectiveness and the robustness of both controllers for the vehicle with respect to path-following control and stability.

The second contribution of this paper is to propose MPC with a feedforward (FF) controller to minimize tracking errors in the lateral position and the yaw angle. To evaluate the effectiveness of the proposed control method, we compare it with LQC with an FF controller. We re-emphasize that the main objective of this paper is a comparative study of path-following control of an autonomous vehicle employing different manoeuvres. To the best of the present authors' knowledge, there has been no comparative study of these three control signal manoeuvres for path-following control of an autonomous vehicle using MPC and LQC techniques, which this paper discusses.

The rest of the paper is organized as follows. The second section describes the vehicle and non-linear tyre model. The linear MPC algorithm and LQC concepts with an FF controller are explained in the third section. The fourth section examines, describes and compares the effectiveness of linear MPC and LQC with an FF controller for vehicle path-following control in a two-lane-change thread scenario based on simulation results. Finally, conclusions and directions for future work are given in the fifth section.

Vehicle model

Double-track model

Figure 1 shows the well-known vehicle model, which is a single-track model based on the simplification that the right wheels and the left wheels are lumped together as a single wheel at the front axle and the rear axle. The simplified vehicle model used in this paper illustrates the motion and dynamics of the vehicle subject to the longitudinal, lateral, yaw and roll motions representing the four degrees of freedom in the model. The longitudinal, lateral and yaw dynamics effects are shown from the top views of the vehicle in Figure 1(a) and (b) for different control manoeuvres, whereas the roll dynamics effect is illustrated from the side view and the front view of the vehicle in Figure 1(c) and Figure 1(d) respectively, together with the notation.

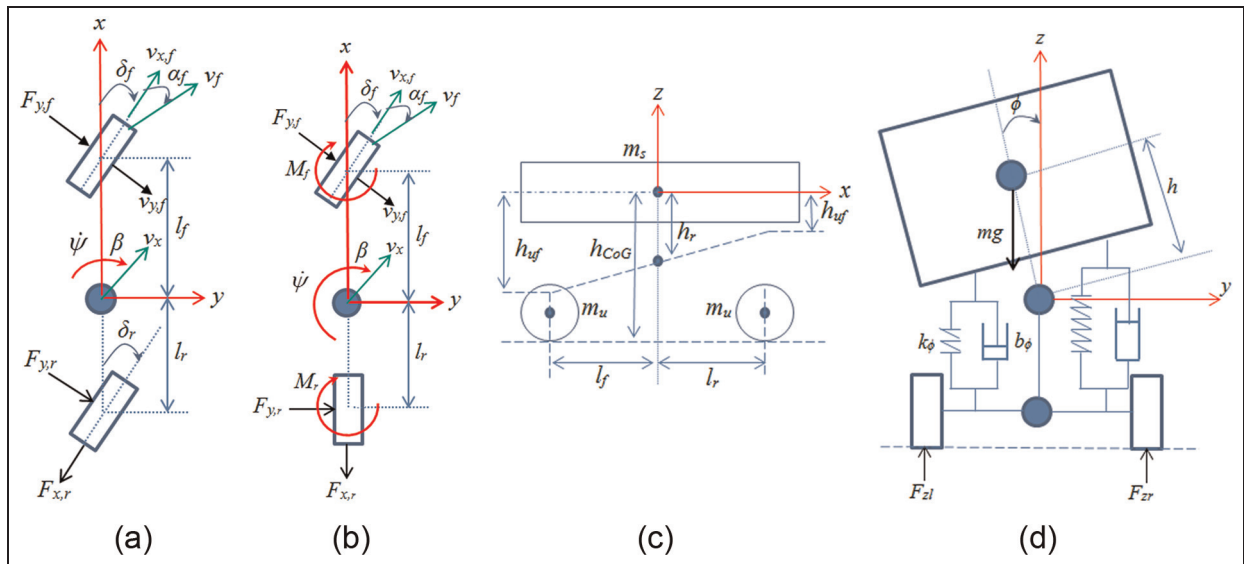


Figure 1. Simplified bicycle model: (a) 4WS; (b) 2WS with DYC; (c) side view; (d) front view.

In this paper, the non-linear vehicle is linearized on the assumption that the vehicle's forward speed is constant. It is assumed that the steering angle, the vehicle's side-slip angle and the roll angle are sufficiently small that they can be neglected. We also assume that the entire vehicle mass is sprung, ignoring the suspension and wheel masses as unsprung masses. This linearized model is a satisfactory approximation for the behaviour of the actual non-linear vehicle model under certain operating conditions. The details of the mathematical calculations for the vehicle model have been presented by Chen and Peng.³²

The longitudinal, lateral, yaw, roll and rotational dynamics of the front wheels and rear wheels representing 8DoFs are described by the differential equations

$$m\ddot{x} = m\dot{y}\dot{\psi} + 2F_{xf} + 2F_{xr} + 2hm\dot{\psi}\dot{\phi} \quad (1a)$$

$$m\ddot{y} = -m\dot{x}\dot{\psi} + 2F_{yf} + 2F_{yr} + hm\ddot{\phi} \quad (1b)$$

$$I_{zz}\ddot{\psi} = 2l_f F_{yf} - 2l_r F_{yr} + I_{xz}\ddot{\phi} + M_z \quad (1c)$$

$$(I_{xx} + mh^2)\ddot{\phi} = mgh\dot{\phi} - 2k_\phi\phi - 2b_\phi\dot{\phi} + mh(\ddot{y} + \dot{\psi}\dot{x}) + I_{xz}\ddot{\psi} \quad (1d)$$

$$J_b\ddot{\omega}_{wi} = -r_w F_{xi} - T_{bi} - b_w\omega_i, i = (f, r) \quad (1e)$$

The equations of motion for the vehicle in an inertial frame described by the $X-Y$ coordinates under the assumption of a small yaw angle may be written as

$$\begin{aligned} \dot{X} &\approx \dot{x} \cos \psi - \dot{y} \sin \psi \\ &\approx v_x - \dot{y} \psi \end{aligned} \quad (2a)$$

$$\begin{aligned} \dot{Y} &\approx \dot{x} \sin \psi + \dot{y} \cos \psi \\ &\approx v_x \psi + \dot{y} \end{aligned} \quad (2b)$$

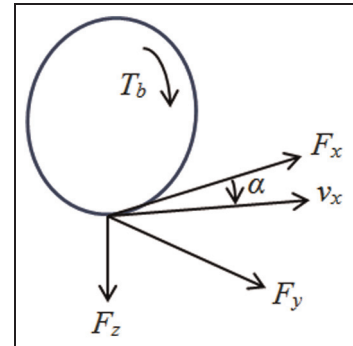


Figure 2. Notation for the tyre model.

Non-linear tyre model

The tyre dynamics must be considered in the vehicle model, since the tyres are the only place of contact that the vehicle has with the road surface. Besides the gravitational and aerodynamic forces, all the forces on the vehicle are transmitted by the tyres and may affect the vehicle chassis, the handling and the stability. Their highly complex and non-linear behaviour must also be reflected in the operating condition of the controller throughout the whole range of longitudinal, lateral and roll manoeuvres. The most commonly used non-linear tyre model, namely the Pacejka³³ model, is a semiempirical model based on analytical considerations and key parameters derived from tyre data measurements and is the model that will be adopted in this paper.

Figure 2 illustrates the notation describing the longitudinal and lateral forces on the tyre and its orientation. The relationships between the longitudinal force, the longitudinal slip ratio of the tyres and the normal load forces for the front wheels and the rear wheels due to the load transfer caused by lateral accelerations are given by the equations

$$F_x = \mu_x(s) F_z \quad (3a)$$

$$F_{zf} = \frac{l_r mg}{2l} - \frac{F_y \phi}{2} - \frac{k_{\phi f} \phi}{t_w} - \frac{b_{\phi f} \dot{\phi}}{t_w} - \frac{h_{uf} F_{yf}}{t_w} - \frac{h_{uf} l_r m g \phi}{t_w l} \quad (3b)$$

$$F_{zr} = \frac{l_f mg}{2l} - \frac{F_y r \phi}{2} - \frac{k_{\phi r} \phi}{t_w} - \frac{b_{\phi r} \dot{\phi}}{t_w} - \frac{h_{ur} F_{yr}}{t_w} - \frac{h_{ur} l_f m g \phi}{t_w l} \quad (3c)$$

The non-linear characteristics of the longitudinal force and the lateral force on the front tyres and the rear tyres are described in the Pacejka tyre model by the relationships (which neglect the self-aligning moment)

$$F_x(s) = D_x \sin \left\{ C_x \tan^{-1} [B_x(1 - E_x)s + E_x \tan^{-1}(B_x s)] \right\} \quad (4a)$$

$$F_y(\alpha) = D_y \sin \left\{ C_y \tan^{-1} [B_y(1 - E_y)\alpha + E_y \tan^{-1}(B_y \alpha)] \right\} \quad (4b)$$

where the parameters B , C , D and E are the constant values of the stiffness factor, the shape factor, the peak value and the curvature factor, which are constant for a given value of the vertical load force. The non-linear kinematics of the tyre slip angles for the front wheels and the rear wheels and the longitudinal slip ratio of the tyre are given by

$$\begin{aligned} \alpha_f &= \frac{v_y + l_f \dot{\psi}}{v_x} - \delta_f \\ \alpha_r &= \frac{v_y - l_r \dot{\psi}}{v_x} - \delta_r \end{aligned} \quad (5a)$$

$$s = \frac{r_w \omega_w}{v_x} - 1, \text{ braking if } r_w \omega_w < v_x \quad (5b)$$

$$s = 1 - \frac{v_x}{r_w \omega_w}, \text{ acceleration if } r_w \omega_w \geq v_x \quad (5c)$$

Control allocation

In this section, the linear MPC and LQC are explained. The basic hierarchical control structure adopted for MPC and LQC is shown in Figure 3. In the control structure illustrated in Figure 3, a 2WS model using only front steering, a 4WS model using front and rear steering or a DYC model producing a reaction moment at the front wheels and the rear wheels are used to control the vehicle so that it follows a given reference trajectory. It includes the vehicle speed, the desired reference trajectory, MPC and a linear vehicle model with a non-linear tyre model. LQC will be implemented in the same way as MPC to facilitate a fair comparison.

Linear MPC

To implement MPC with a receding-horizon control strategy, the following strategies are adopted.

1. A dynamic process model is used to predict the behaviour of the plant and future plant outputs

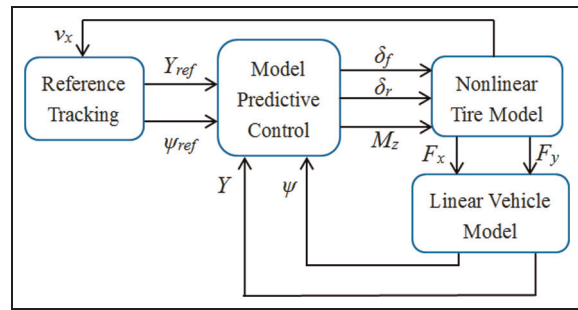


Figure 3. Predictive control structure.
MPC: model predictive control.

based on the latest and past observations of the system inputs and outputs.

2. The control signal inputs are calculated by minimizing the tracking error between the predicted output and the desired trajectory signal to keep the process following the trajectory as closely as possible, taking into account the objective function and constraints.
3. Only the first control signal is implemented on the plant, whereas others are rejected at the next sampling instant where the future output is known.
4. Step 1 is repeated with the updated value, and all orders are updated.

For simplicity, the MPC is designed on the basis of a simple 2DoF lateral yaw motion by linearizing the equations from the vehicle and tyre models as explained and defined in equations (1) to (5), giving the basic equations of free-rolling linear vehicle motion without braking or acceleration as

$$\begin{aligned} \hat{m} \ddot{v}_y &= \frac{1}{v_x} \left\{ -(C_r + C_f) v_y + \left[(C_r l_r - C_f l_f) - \hat{m} v_x^2 \right] \dot{\psi} \right\} \\ &\quad + (C_f \delta_f + C_r \delta_r) \end{aligned} \quad (6a)$$

$$\begin{aligned} \hat{I}_{zz} \ddot{\phi} &= \frac{1}{v_x} \left[(C_r l_r - C_f l_f) v_y - (C_f l_f^2 + C_r l_r^2) \dot{\psi} \right] \\ &\quad + C_f l_f \delta_f - C_r l_r \delta_r + M_z \end{aligned} \quad (6b)$$

The relationship between the cornering force and the slip angle of the tyres is linear, whereas the slip angle is small. The lateral forces F_{yi} on the front tyres and the rear tyres are treated as proportional to the slip angle α_i of the tyres as described by

$$\begin{aligned} F_{yf} &= C_f \alpha_f \\ F_{yr} &= C_r \alpha_r \end{aligned} \quad (7)$$

where C_f and C_r are the constants representing the linear cornering stiffnesses of the front tyres and the rear tyres respectively.

For the DYC, the reaction moment occurring at the front wheels and the rear wheels due to the

steering-angle effect (as an external yaw moment M_z) can be approximated as

$$\begin{aligned} M_f &\approx 2 l_f C_f M_z \\ M_r &\approx 2 l_r C_r M_z \end{aligned} \quad (8)$$

with the normalized vehicle mass and the normalized moment of inertia being given by

$$\begin{aligned} \hat{m} &= \frac{m}{\mu} \\ \hat{I}_{zz} &= \frac{I_{zz}}{\mu} \end{aligned} \quad (9)$$

The vehicle motion in equation (6) can be represented in state-space form as

$$\begin{aligned} \dot{x} &= Ax + B_1 u + B_2 w_{des} \\ y &= Cx + Du \end{aligned} \quad (10)$$

where $x \in \mathbb{R}^x$, $u \in \mathbb{R}^u$, $w_{des} \in \mathbb{R}^w$ and $y \in \mathbb{R}^y$ are the state vectors, the control input vectors, the desired trajectory vectors and the measured output vectors respectively. We define

$$\begin{aligned} x &= [v_y \ Y \ \dot{\psi} \ \psi]^T \\ u &= [\delta_f], \quad [\delta_f \ \delta_r]^T, \quad [\delta_f \ M_z]^T \\ w_{des} &= [Y_{des} \ \psi_{des}]^T \end{aligned} \quad (11a)$$

$$y = [Y \ \dot{\psi} \ \psi]^T \quad (11b)$$

The state vectors represent the states for the lateral velocity, the lateral position, the yaw rate and the yaw angle, and the output vectors represent the lateral position, the yaw angle and the yaw rate.

We define the front steering angle, the rear steering angle and DYC as the inputs to the system. Thus, the vehicle motion in equation (10) can be represented in discrete state-space form as MPC is designed in discrete form and is given by

$$x_l(k+1|k) = A_l x_l(k|k) + B_l u_l(k|k) \quad (12a)$$

$$y_l(k|k) = C_l x_l(k|k) + D_l u_l(k|k) \quad (12b)$$

where $x_l(k|k)$ is the state vector at time step k and $x_l(k+1|k)$ is the state vector at time step $k+1$, with $x_l(k|k) \in \mathbb{R}^{x_l(k|k)}$, $u_l(k|k) \in \mathbb{R}^{u_l(k|k)}$ and $y_l(k|k) \in \mathbb{R}^{y_l(k|k)}$, which are the state vectors, the control input vectors and the measured output vectors respectively.

For 2WS, 4WS and 2WS with DYC, the control signals for the systems with the same tuning control parameters are

$$u_l(k) = [\delta_f] \quad (13a)$$

$$u_l(k) = [\delta_f \ \delta_r]^T \quad (13b)$$

and

$$u_l(k) = [\delta_f \ M_z]^T \quad (13c)$$

respectively.

Because the controller is designed on the basis of a simple 2DoF bicycle model, neglecting roll dynamics and considering a linear tyre model, it is impossible for the controller to track and follow a given or desired trajectory perfectly or accurately. However, the controller is designed to achieve the aim of a double-lane change scenario for different control manoeuvres through simulations. The objective of the predictive control system is to bring the predicted output as close as possible to the reference signal within a predictive horizon, where we assume that the reference signal remains constant in the optimization window. It should also be noted that the objective is to find the optimal control input vector $\Delta\hat{u}_l(k+i|k)$ such that an error function between the predicted output and the reference signal is minimized. The control objectives are typically a trade-off between how well the controller tracks the output reference and how much input action it uses. The optimization of the predictive control system will be solved by minimizing a cost function given by

$$\begin{aligned} J_{mpc}(x(k), U_k) = & \sum_{i=1}^{H_p} \|\hat{y}_l(k+i|k) - w_{ref}(k+i|k)\|_{Q_i}^2 \\ & + \sum_{i=0}^{H_c-1} \|\Delta\hat{u}_l(k+i|k)\|_{R_i}^2 \end{aligned} \quad (14)$$

Here, the first summation refers to minimizing the trajectory of the tracking error between the predicted outputs $\hat{y}_l(k+i|k)$ ($i = 0, \dots, n$) and the output reference signal $w_{ref}(k+i|k)$ ($i = 0, \dots, n$). The second summation reflects the penalty on the control signal effort due to the front steering angle, $\Delta\hat{u}_l(k+i|k)$ ($i = 0, \dots, n$), in the case of the 2WS control manoeuvre. Here, $w_{ref}(k+i|k)$ is the reference value of the lateral position and the yaw angle. The variation in the front steering angle $\Delta\hat{u}_l(k+i|k)$ can be obtained by making the cost function as small as possible. The weight matrices Q_i and R_i are diagonal matrices that can be adjusted for the desired closed-loop performance. We have defined Q_i as the state tracking weight because the error $\hat{y}_l(k+i|k) - w_{ref}(k+i|k)$ can be made as small as possible by increasing Q_i . Similarly, R_i is defined as the input tracking weight, and the variation in the input is reduced to slow the response of the system by increasing R_i . The predictive and control horizons are usually assumed to satisfy $H_p \geq H_c$.

The inherent physical limitations on the capacity of control actuators or on the rate of control actuators give rise to the hard constraints on the input and on the input rate. Both the constraints have a profound impact on the stabilization of a given initial condition and the performance of the closed-loop systems. The input constraints are usually applied to avoid actuator saturation and are imposed to arrest an aggressive control move. Thus, the second constraints add stability to the system. The optimization of the predictive control system, taking into account the constraints on the actuators due to

physical reasons (i.e. the ranges of the front-tyre torque, the rear-tyre torque and the moment torque), is formulated as

$$\begin{aligned} \min_{\Delta U_l} & [J_{mpc}(x_l(k), \Delta U_l(k))] \\ \text{subject to} \\ \dot{x}_l(k+1|k) &= A_l x_l(k|k) + B_l u_l(k|k) \\ \dot{x}_l(k+2|k) &= A_l \dot{x}_l(k+1|k) + B_l \dot{u}_l(k|k) \\ &\vdots \\ \dot{x}_l(k+i|k) &= A_l \dot{x}_l(k+i-1|k) + B_l \dot{u}_l(k+i-1|k) \\ \delta_{f,min} \leq \hat{u}_l(k+i|k) &\leq \delta_{f,max}, \quad 2WS \\ \delta_{r,min} \leq \hat{u}_l(k+i|k) &\leq \delta_{r,max}, \quad 4WS \\ M_{z,min} \leq \hat{u}_l(k+i|k) &\leq M_{z,max}, \quad DYC \\ \Delta \delta_{f,min} \leq \Delta \hat{u}_l(k+i|k) &\leq \Delta \delta_{f,max} \\ \Delta \delta_{r,min} \leq \Delta \hat{u}_l(k+i|k) &\leq \Delta \delta_{r,max} \\ \Delta M_{z,min} \leq \Delta \hat{u}_l(k+i|k) &\leq \Delta M_{z,max}, \quad i = 1, \dots, H_p \end{aligned} \quad (15)$$

The maximal slip angles $\alpha_{f,max}$ and $\alpha_{r,max}$ of the tyres are detected where the maximal tyre force is achieved in order to prevent extreme saturation of the lateral tyre force. By knowing an upper-bound angle limit and a lower-bound angle limit as functions of the slip angle of the vehicle and a slip angle limit of the tyres, the maximal front steering-angle limit and the rear steering-angle limit can be derived as

$$\begin{aligned} \delta_{f,max}(k) &= \alpha_{f,max} + \frac{v_y - l_f \dot{\psi}}{v_x} \\ \delta_{r,max}(k) &= \alpha_{r,max} + \frac{v_y + l_r \dot{\psi}}{v_x} \end{aligned} \quad (16)$$

The inequality of the slip angles of the tyres, $-\alpha_{lim} < \alpha_f < +\alpha_{lim}$, indicates that the steering angle δ_f of the front wheels may be held within a bound of the vehicle side-slip angle β_f to avoid the saturation region of the lateral tyre force. Thus, these bounds are determined once at time k such that $\alpha_{f,max}(k+i|k)$ is equal to a constant where, before the upper bound and the lower bound are defined, the linearization of the non-linear tyre model (4) is investigated at the operating point $\alpha_{f,0}$, $F_{yf,0}$ as given by

$$F_{yf} = (\alpha_f - \alpha_{f,0}) k_{af} + F_{yf,0} \quad (17)$$

where k_{af} is the linearization coefficient.³⁴ The same applies for the rear steering angle. For the case of DYC, when lateral force saturation of both the front tyres and the rear tyres is reached, an additional yaw moment M_z is used in order to reach the yaw rate tracking goal.

The optimization problem (15) is based on the linear system (10), where the optimization problem (15) can be recast as a quadratic program (QP) or a linear program if the function (14) is convex linear or quadratic (details can be found in the paper by Borrelli et al.³¹). Then, the resulting model predictive controller for the

linear system will solve the problem (15) at each time step. Once a solution, namely u_k^* , to problem (15) was obtained, the input command is computed as

$$u(k) = u(k-1) + \Delta u_k^* \quad (18)$$

At the next time step, the linear model is computed on the basis of new state and input measurements, which means that the new QP problem (15) is being solved over a shifted horizon. Finally, an optimal input is then calculated for the next time step (instead of the immediate time step) by solving a convex optimization problem at each time step.

In general, the stability of the presented control scheme is difficult to prove. On the basis of the accurate analysis of the non-linearities of the vehicle, we obtained a stable and performing controller by a proper choice of the cost function and the system constraint. In particular, without the constraints, the performance of the linear model predictive controller is not acceptable and sometimes unstable. This is because a simple linear model is not able to predict the change in the slope of the tyres' characteristics. To overcome this issue we add constraints to the optimization problem, in order to prevent the system from entering into a non-linear and possibly unstable region of the tyres' characteristics. Thus, the slip angle constraints (16) of the tyres are used to maintain the stability of the vehicle. It is well known that the stability is not ensured by the MPC laws (15) and (17), since our problem is a linear problem. Thus, for non-linear MPC, usually the problem is augmented with a terminal cost and terminal constraint set to ensure closed-loop stability,³⁵ and that is beyond the scope of this work.

LQC

To allow a fair comparison of the tracking responses with those from MPC, LQC is also based on the linearized vehicle equations (6) with a quadratic cost function. The aim of this approach, called linear quadratic tracking, is to track and follow the desired trajectory as closely as possible, with the linear quadratic solution.^{36,37} We denote the control error by $e_{er}(t)$, the desired trajectory by $w_{des}(t)$ and the performance output by $y_l(t)$, with these being related by

$$e_{er}(t) = w_{des}(t) - y_l(t) \quad (19)$$

The integral error is then given by

$$e_e = \int_0^t e_{er}(t) dt \quad (20)$$

which is introduced as a new state to the dynamic system (6) as given in state space by

$$\begin{bmatrix} \dot{e}_e \\ \dot{x}_l \end{bmatrix} = \begin{bmatrix} 0 & -I \\ 0 & A_l \end{bmatrix} \begin{bmatrix} e_e \\ x_l \end{bmatrix} + \begin{bmatrix} 0 \\ B_l \end{bmatrix} u_l + \begin{bmatrix} I \\ 0 \end{bmatrix} w_{des} \quad (21)$$

which can be simplified as $\dot{x}_{lq} = A_{lq}x_{lq} + B_{lq}u_{lq} + E_{lq}w_{des}$. Thus, the new error for the system (21) can be defined as

$$\begin{aligned}\varepsilon &= \begin{bmatrix} \varepsilon \\ \varepsilon_e \end{bmatrix} \\ &= Mw_{des} + Hx_{lq}\end{aligned}\quad (22)$$

With an infinite-horizon problem, the cost function is given by

$$J_{lqc} = \min_u \left\{ \int_0^{\infty} [e^T(t)Q_{lq}e(t) + u_{lq}^T(t)R_{lq}u_{lq}(t)] dt \right\}$$

subject to

$$\begin{aligned}\dot{\varepsilon}(t) &= A_{lq}\varepsilon(t) + B_{lq}u_{lq}(t) \\ \varepsilon(0) &= \varepsilon_0\end{aligned}\quad (23)$$

where Q_{lq} and R_{lq} are the positive-definite weighting matrices on the tracking error and on the input error respectively. We try to find the control $u_{lq}(t)$ that will regulate the system at zero by tuning Q_{lq} and R_{lq} . The optimal input state feedback controller K_{opt} is obtained by minimizing the cost function

$$K_{opt} = \begin{bmatrix} -R_{lq}^{-1}B_{lq}^T P_{11} & -R_{lq}^{-1}B_{lq}^T P_{12} \end{bmatrix} \quad (24)$$

where P_{11} and P_{12} are the unique positive-definite solutions to the algebraic Riccati equation for an infinite-horizon linear quadratic problem

$$A_{lq}^T P_e + P_e A_{lq} - P_e B_{lq} R_{lq}^{-1} B_{lq}^T P_e + Q_{lq} = O \quad (25)$$

where

$$Q_{lq} = \begin{bmatrix} C^T Q_{11} C & 0 \\ 0 & Q_{22} \end{bmatrix} \quad (26)$$

and O is the zero matrix. The solutions of the Riccati differential equation are

$$P_e = P_e^T = \begin{bmatrix} P_{11} & P_{12} \\ P_{21}^T & P_{22} \end{bmatrix} > 0 \quad (27)$$

Here, the FF gain K_s , which is designed for target tracking, and the feedback gain K_f are given by

$$K_s = \left[-C_{lq}(A_{lq} + B_{lq}K_{opt})^{-1} B_{lq} \right]^{-1} \quad (28a)$$

and

$$K_f = C_{lq}(A_{lq} + B_{lq}K_{opt})^{-1} \quad (28b)$$

respectively with the control law being given by

$$u_{lq}(t) = -K_s x_{lq} - K_f w_{des} \quad (29)$$

Once the algebraic Riccati equation has been solved, the optimal gains can be computed from equation (28). The problem now becomes how to choose the weighting matrices Q and R so that a good response is obtained

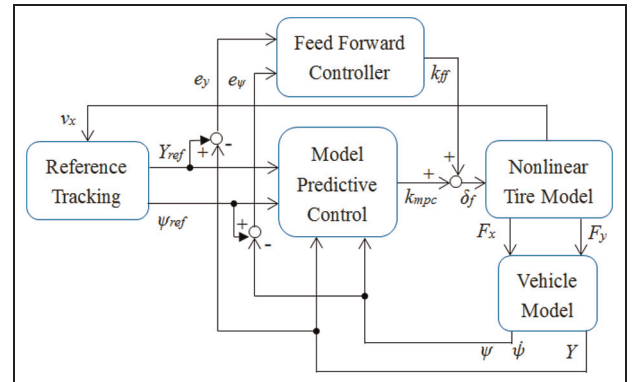


Figure 4. Predictive control with an FF controller.

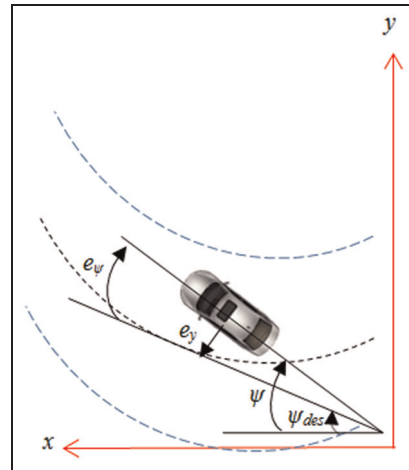


Figure 5. Vehicle motion with respect to the lane.

without exceeding the bandwidth and position limitations of the actuators, i.e. without so-called saturation.

MPC with an FF controller

In this subsection, we propose MPC with an FF controller for path-following control of an autonomous sport utility vehicle, for the active front steering control manoeuvre as shown in Figure 4. MPC is designed to track and follow a given trajectory as closely as possible, while the FF controller is adopted in order to reduce the tracking errors between the desired outputs and the real outputs, thus enhancing the vehicle stability and the handling manœuvrability.

The trajectory errors of the vehicle motion, with respect to the centre lane of the road as shown in Figure 5, are given by

$$e_\phi = \psi - \psi_{des} \quad (30a)$$

$$\dot{e}_y = \dot{y} \cos(e_\psi) + \dot{x} \sin(e_\psi) \quad (30b)$$

$$\dot{e}_x = -\dot{y} \sin(e_\psi) + \dot{x} \cos(e_\psi) \quad (30c)$$

The acceleration is along the Y axis, and the side-slip angle of the vehicle body, under small-angle

assumptions, is related to the lateral position error and the yaw angle error by

$$\begin{aligned} a_y &= \dot{y} + \dot{\psi} v_x \\ \dot{y} &= \dot{e}_y - e_\psi v_x \end{aligned} \quad (31)$$

In Figure 4, the state feedback from the MPC with an FF controller is adopted here to stabilize the vehicle for a known trajectory and to correct the errors that accumulated owing to unmodelled vehicle dynamics, disturbances or parameter uncertainties. A model predictive controller is used for tracking purposes owing to the advantages for multi-variable and constraint systems. An FF controller is adopted for minimizing tracking errors and to ensure zero steady-state errors because of its simplicity, thus enhancing the vehicle stability. A driver steering controller using a general linear quadratic regulator formulation was derived by Sharp and Valtetsiotis,³⁸ while MPC was employed by Cole et al.³⁹ and MacAdam,⁴⁰ where the solution of a cost function results in an MPC steering law, based on state feedback and future path preview for a discrete domain controller, and given by

$$k_{mpc}(k) = -[k_k \ x(k)\Omega \quad k_k] \begin{bmatrix} x(k) \\ T_k \end{bmatrix} \quad (32)$$

where Ω is the free response matrix of the dynamics system, k_k is the controller preview gain vector derived using MPC formulation and T_k is the preview vector. Let us assume that the steering controller is obtained from the state feedback of MPC in equation (32) where the FF controller term is

$$u(k) = \delta_f(k) = -k_{mpc} x(k) + k_{ff} \quad (33)$$

From system (10), the eigenvalues of the closed-loop matrix $A - B_1 k_{mpc}$ can be placed at any desired location. Let us assume that the longitudinal speed of the vehicle is constant. Then, the closed-loop system is given by

$$\dot{x} = (A - B_1 k_{mpc})x + B_1 k_{ff} + B_2 w_{des} \quad (34)$$

For simplicity, we assume zero initial conditions and, taking the Laplace transform ℓ of equation (34), we find that

$$X(s) = [sI - (A - B_1 k_{mpc})]^{-1} [B_1 \ell(k_{ff}) + B_2 \ell(w_{des})] \quad (35)$$

For ease of understanding, let us assume that here $w_{des} = \dot{\phi}_{des} = v_x / R_w$. Then, with a small-angle assumption, a constant forward speed and a constant radius of curvature, we obtain

$$\begin{aligned} \ell(w_{des}) &= \frac{v_x}{sR_w} \\ \ell(k_{ff}) &= \frac{k_{ff}}{s} \end{aligned} \quad (36)$$

Based on the final-value theorem, the steady-state tracking error is given by

$$\begin{aligned} x_{ss} &= \lim_{t \rightarrow \infty} [x(t)] \\ &= \lim_{s \rightarrow 0} [sX(s)] \\ &= - (A - B_1 k_{mpc})^{-1} (B_1 k_{ss} + B_2 w_{des}) \end{aligned} \quad (37)$$

The state-space model in tracking-error variables is therefore given by

$$\begin{bmatrix} \dot{e}_y \\ \ddot{e}_y \\ \dot{e}_\psi \\ \ddot{e}_\psi \end{bmatrix} = \begin{bmatrix} 0 & 1 & 0 & 0 \\ 0 & -\frac{C_f + C_r}{mv_x} & \frac{C_f + C_r}{m} & -\frac{C_f l_f - C_r l_r}{mv_x} \\ 0 & 0 & 0 & 1 \\ 0 & -\frac{C_f l_f - C_r l_r}{I_{zz} v_x} & \frac{C_f l_f - C_r l_r}{I_{zz}} & -\frac{C_f l_f^2 + C_r l_r^2}{I_{zz} v_x} \end{bmatrix} \begin{bmatrix} e_y \\ \dot{e}_y \\ e_\psi \\ \dot{e}_\psi \end{bmatrix} \\ + \begin{bmatrix} 0 \\ -\frac{C_f l_f - C_r l_r}{mv_x} - v_x \\ 0 \\ -\frac{C_f l_f^2 + C_r l_r^2}{I_{zz} v_x} \end{bmatrix} \dot{\psi}_{des} + \begin{bmatrix} 0 \\ \frac{C_f}{m} \\ 0 \\ \frac{C_f l_f}{I_{zz}} \end{bmatrix} \delta_f \quad (38)$$

Again, for simplicity, we evaluate equation (37) using the symbolic toolbox in MATLAB, yielding the steady-state errors

$$x_{ss} = \begin{bmatrix} -\frac{mv_x^2}{k_{mpc1} R_w l} \left(\frac{l_r}{C_f} - \frac{l_f}{C_r} + \frac{l_f k_{mpc3}}{C_r} \right) - \frac{l - l_r k_{mpc3}}{k_{mpc1} R_w} + \frac{k_{ff}}{k_{mpc1}} \\ 0 \\ \frac{-C_r l_f l_r - C_r l_r^2 + l_f m v_x^2}{C_r R_w l} \\ 0 \end{bmatrix} \quad (39)$$

The steady-state lateral position error can be made zero if the FF steering angle is chosen as

$$k_{ff} = \frac{mv_x^2}{R_w l} \left(\frac{l_r}{C_f} - \frac{l_f}{C_r} + \frac{l_f k_{mpc3}}{C_r} \right) + \frac{l}{R_w} - \frac{l_r k_{mpc3}}{R_w} \quad (40)$$

However, k_{ff} cannot influence the steady-state yaw angle error irrespective of how the k_{ff} steering angle is chosen, as can be seen from equation (39). The steady-state yaw angle error from equation (39) can be written as

$$e_\psi = \frac{-C_r l_f l_r - C_r l_r^2 + l_f m v_x^2}{C_r R_w l} \quad (41)$$

If we rearrange equations (40) and (41), then the FF steering angle is given by

$$k_{ff} = \frac{l}{R_w} + k_{mpc3} e_\psi + \frac{mv_x^2}{R_w l} \left(\frac{l_r}{C_f} - \frac{l_f}{C_r} \right) \quad (42)$$

Thus, the steady-state steering angle for the zero-lateral-position error is given by

$$k_{ss} = \frac{l}{R_w} + \frac{mv_x^2}{R_w l} \left(\frac{l_r}{C_f} - \frac{l_f}{C_r} \right) \quad (43)$$

From equation (41), we may rewrite and rearrange the equation in order to achieve the error with a zero steady-state yaw angle if the vehicle parameters and the vehicle speed are chosen as

Table 1. Parameters of the Ford Taurus sport utility vehicle.

Parameter	Value
m	1542
I_{xx}	670
I_{zz}	2786
I_{xz}	166
I_f	0.92
I_r	1.77
h	0.55
t_w	1.02
b_ϕ	4500
k_ϕ	72,500
C_f	106,000
C_r	88,000
G	9.8

$$\frac{l_r}{R_w} = \frac{l_f m v_x^2}{C_r R_w l} \quad (44)$$

where this happens at particular vehicle speeds, and this speed is independent of the path curvature. Further details have been given by Rajamani.⁴¹

Simulation results

Scenario description

The linear MPC and LQC presented above were implemented in simulations for path-following vehicle control in a double-lane-change scenario. The double-lane-change manoeuvre approximates an emergency manoeuvre case and generally demonstrates the agility and capabilities of a vehicle in terms of the lateral dynamics. During such a manoeuvre, understeering, oversteering or even rollover may occur. For these scenarios, Table 1 shows the model parameters for a Ford Taurus sport utility vehicle. Simulations were performed using the MPC Toolbox in MATLAB and Simulink software. In this paper, the predictive controller was used to minimize the deviation of the vehicle from the target path to achieve the main aim, namely to follow the desired or reference trajectory as closely as possible. The controllers based on simple 2DoF vehicle motion were compared with each other for a non-linear vehicle system at a low forward speed (10 m/s) and a high forward speed (25 m/s) on an ideal road friction surface, and at a medium forward speed (20 m/s) on a low-road-friction surface (wet earth with snow; $\mu = 0.3$).

In this paper, both the model predictive controller and the linear quadratic controller were designed and implemented in the simulation scenarios, with the parameters and conditions given in Tables 2 and 3. The weighting matrices for the inputs and outputs of MPC and LQC were based on a trial-and-error process, where the main target here is to achieve the zero-lateral-position error rather than the zero-yaw-angle error. Here, the weighting matrices were selected on the basis of the best-response outputs by first tuning the outputs gain parameter, which was then followed by tuning the input gains parameter.

Table 2. Parameters of the controller.

Parameter	Value
H_p	20
H_c	9
T_s	0.05
$\delta_f \delta_r$	± 30
$\Delta \delta_f \Delta \delta_r$	± 20
M_z	± 2000
ΔM_z	± 1500
T	15

Table 3. Parameters of the weighting matrices of the controllers.

Control manoeuvres		MPC	LQC
2WS	$v_x = 10 \text{ m/s}, \mu = 1$	$R_1 = 0.1$	$R_{lq} = 5$
		$Q_{11} = 2.05$	$Q_{lq1} = 10$
		$Q_{22} = 0.5$	$Q_{lq2} = 1.5$
	$v_x = 25 \text{ m/s}, \mu = 1$	$R_1 = 0.1$	$R_{lq} = 5$
		$Q_{11} = 5.25$	$Q_{lq1} = 20$
		$Q_{22} = 0.5$	$Q_{lq2} = 2.5$
	$v_x = 20 \text{ m/s}, \mu = 0.3$	$R_1 = 0.1$	$R_{lq} = 5$
		$Q_{11} = 2.65$	$Q_{lq1} = 12$
		$Q_{22} = 0.65$	$Q_{lq2} = 2.8$
4WS	$v_x = 10 \text{ m/s}, \mu = 1$	$R_1 = 0.1$	$R_{lq1} = 5$
		$R_2 = 0.1$	$R_{lq2} = 5$
		$Q_{11} = 2.85$	$Q_{lq1} = 4.65$
		$Q_{22} = 0.2$	$Q_{lq2} = 1.55$
	$v_x = 25 \text{ m/s}, \mu = 1$	$R_1 = 0.1$	$R_{lq1} = 5$
		$R_2 = 0.1$	$R_{lq2} = 5$
		$Q_{11} = 3.15$	$Q_{lq1} = 14.5$
		$Q_{22} = 0.5$	$Q_{lq2} = 2.55$
	$v_x = 20 \text{ m/s}, \mu = 0.3$	$R_1 = 0.1$	$R_{lq1} = 5$
2WS + DYC	$v_x = 10 \text{ m/s}, \mu = 1$	$R_1 = 0.1$	$R_{lq1} = 5$
		$R_2 = 0.1$	$R_{lq2} = 5$
		$Q_{11} = 2.15$	$Q_{lq1} = 5$
		$Q_{22} = 0.5$	$Q_{lq2} = 1.5$
	$v_x = 25 \text{ m/s}, \mu = 1$	$R_1 = 0.1$	$R_{lq1} = 5$
		$R_2 = 0.1$	$R_{lq2} = 5$
		$Q_{11} = 4.55$	$Q_{lq1} = 10.4$
		$Q_{22} = 0.5$	$Q_{lq2} = 2.55$
	$v_x = 20 \text{ m/s}, \mu = 0.3$	$R_1 = 0.1$	$R_{lq1} = 5$

MPC: model predictive control; LQC: linear quadratic control; 2WS: two-wheel steering; 4WS; four-wheel steering; DYC: direct yaw moment control.

The path-following tracking error is a measure of how closely the output responses follow the reference trajectory and is a measure of the deviation from the benchmark. In this paper, we use the r.m.s. formula for the standard deviation of the tracking error given by

$$e_t = \sqrt{\text{Var}(y - r_i)} = \sqrt{\frac{1}{n-1} \sum (y - r_i)^2} \quad (45)$$

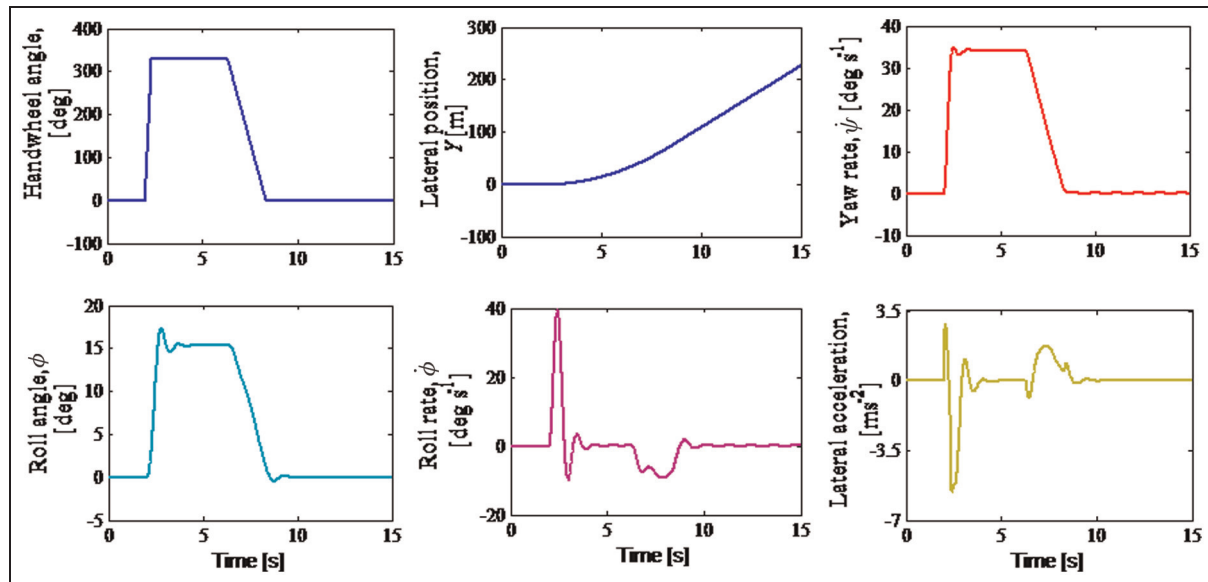


Figure 6. Vehicle manoeuvre test of a J-turn at 20 m/s.

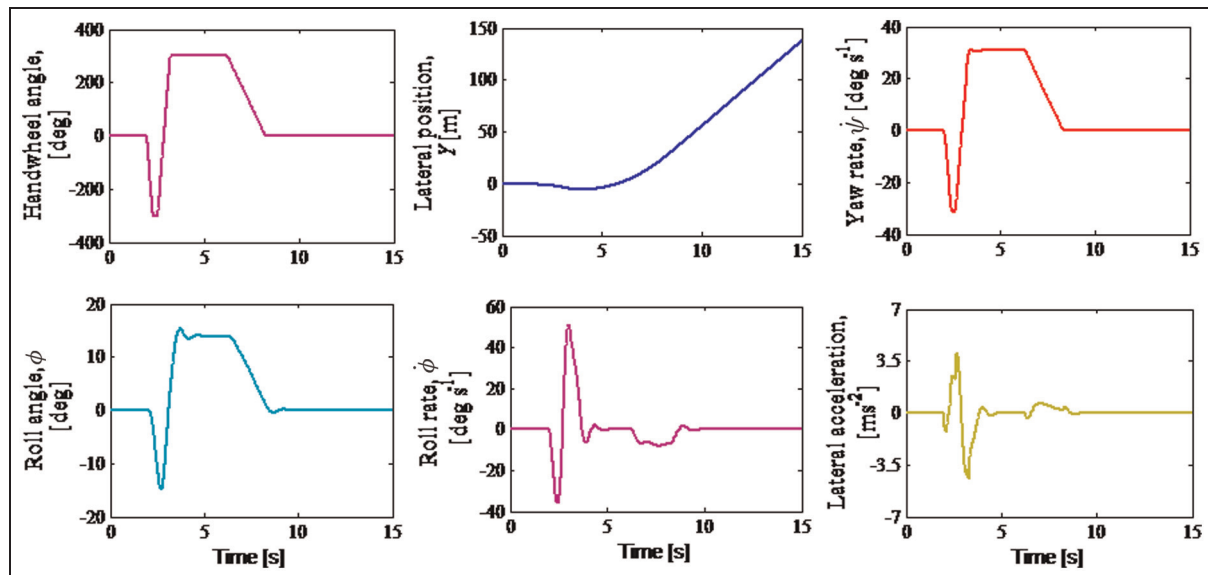


Figure 7. Vehicle manoeuvre test of a roll rate feedback fishhook at 20 m/s.

where n is the number of time periods, y is the measured output and r_i is the reference output.

Results and discussion

Before we started to consider the main objective, we carried out a vehicle manoeuvres test in order to strengthen the credibility of the paper. As most vehicle engineers know, the most common handling manoeuvres used for a vehicle test are J-turn, fishhook and double-lane-change⁴² which are representative of on-road manoeuvres where the vehicle is not tripped (caused by forces from an external object, such as a kerb or a collision with another vehicle). These can be described as follows. The J-turn test is a single steering

manoeuvre, where, following a sudden turn, the steering wheel is then held fixed for the remainder of the test. A fishhook test is a steering reversal manoeuvre, where the vehicle turns with the steering angle changing from 0° to -270° and then from -270° to 600°. The last test is the double-lane-change test which is an avoidance test; this represents a changing vehicle path based on pre-determined cone placement in the road. In this paper, we performed only the NHTSA J-turn and roll rate feedback fishhook test for vehicle validation purposes in the open-loop simulations, as shown in Figures 6 and 7. In these tests, we set the vehicle speed at 20 m/s which is suitable for both tests with a road surface coefficient of 1. Based on the vehicle responses for the yaw rate, the roll rate and the lateral acceleration, it is proved

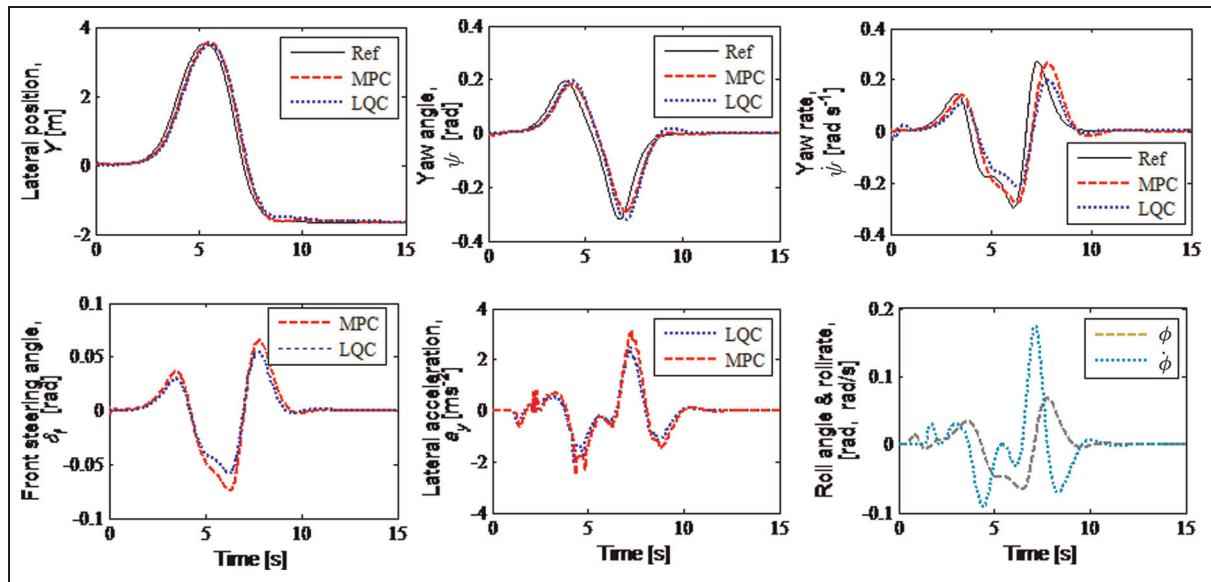


Figure 8. Vehicle manoeuvre by 2WS at 10 m/s.

Ref: reference; MPC: model predictive control; LQC: linear quadratic control.

and shown that the vehicle model is validated and corrected; thus, it can be implemented for controller design.

Since our research is conducted through a simulation process, it is necessary to validate the vehicle model through manoeuvre tests. Another way to strengthen the proposed control methods is to compare the proposed controller with another controller. This way, we are comparing two different controls for the same aims and target, in order to validate and prove that the methods used are sufficiently accurate. Currently, we are developing the vehicle prototype for our next study on real implementation. To facilitate a comparison of the robustness values and the performances of both controllers in stabilizing the vehicle at a chosen speed along the desired trajectory, the controller tuning parameters from Tables 2 and 3 were selected for all situations and conditions of vehicle manoeuvres.

First, we performed a vehicle simulation test under ideal road surface friction coefficients (dry asphalt; $\mu = 1$) at a constant low forward speed of 10 m/s. The MPC and LQC weight tuning parameters are listed in Table 3. We evaluated the robustness values of the controllers for the output responses by comparing the performances of 2WS, 4WS and 2WS with DYC manoeuvres at a forward speed of 10 m/s, as shown in Figure 8, Figure 9 and Figure 10 respectively. The controller tracking errors, which are based on equation (45) for the lateral position and the yaw angle responses, are summarized in Table 4. From Figure 10, for the lowest-speed manoeuvres and with a high road adhesion coefficient, there was not much difference between the manoeuvre controllers; both controllers gave a perfect response when following a given trajectory and maintaining the vehicle stability. It can be seen that, for 4WS and 2WS with DYC manoeuvres,

the rear steering angle and the direct yaw moment are almost unused, since the front steering can provide sufficient control ability. This may be partly because the rear steering and DYC were not used in lower-speed manoeuvres.

In these scenarios, of the three control manoeuvres, the 2WS with DYC performed slightly better (in particular, the yaw angle and the yaw rate responses) followed by 4WS, and finally 2WS, for which the lateral position and the yaw angle look almost identical. In this situation, the figures show that the rear steering of the 4WS manoeuvre is going in the opposite direction from the front steering in order to stabilize the vehicle along the trajectory while, for control under 2WS with DYC, it is used with very little torque because the yaw outputs were successful in tracking and following a given trajectory closely. In the low-forward-speed scenario, both controllers were successfully implemented for all manoeuvre controls because the roll dynamics do not have much influence during low-speed manoeuvres. Furthermore, at low vehicle speeds, all manipulated inputs are under the constraints of the front steering angle, the rear steering angle or DYC.

Next, we simulated the motion of the vehicle at a high forward speed (chosen as 25 m/s) and neglected the road surface friction (which was chosen as dry concrete; $\mu = 1$). We evaluated the robustness values of the controllers for the output response by comparing the performances of 2WS, 4WS and 2WS with DYC manoeuvres as shown in Figure 11, Figure 12 and Figure 13 respectively. It can be seen clearly from these figures that, for the model predictive controller, the trajectory tracking responses for the lateral position and the yaw angle were similar for all control manoeuvres, and it was possible to track and follow a given trajectory successfully. The lateral position responses were

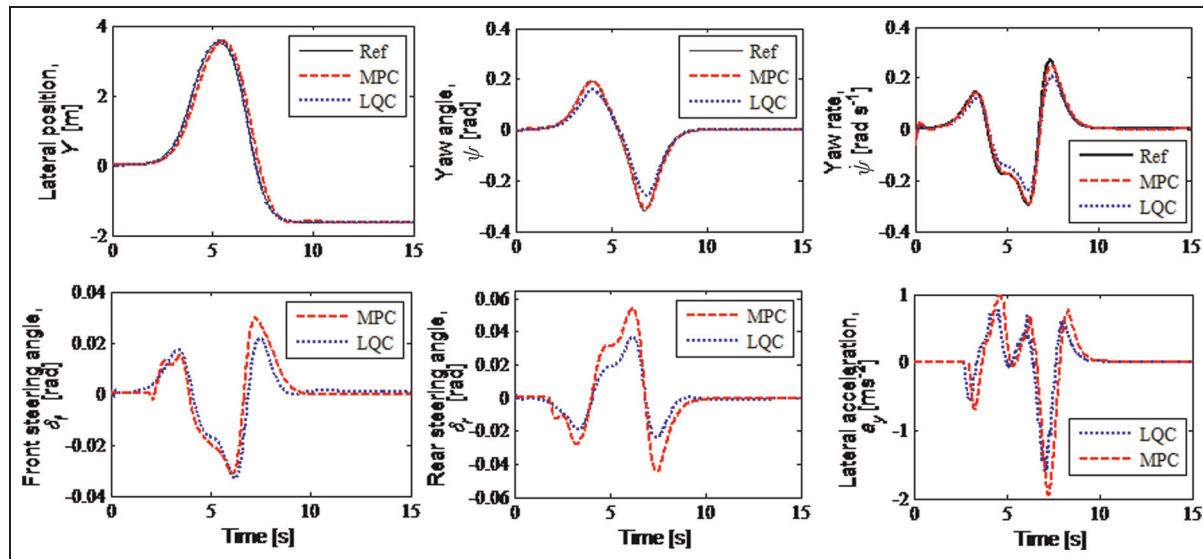


Figure 9. Vehicle manoeuvre by 4WS at 10 m/s.

Ref: reference; MPC: model predictive control; LQC: linear quadratic control.

Table 4. Path-following tracking errors without road-surface friction $\mu = 1$.

Vehicle speed (m/s)	Manoeuvre control	LQC		MPC	
		Y (m)	$\dot{\psi}$ (rad)	Y (m)	$\dot{\psi}$ (m)
10	2WS	0.0798	0.0198	0.0812	0.0081
	4WS	0.0768	0.0165	0.0810	0.0058
	2WS + DYC	0.0772	0.0163	0.0810	0.0054
25	2WS	0.0882	0.7645	0.0994	0.2146
	4WS	0.0834	0.8484	0.0838	0.0782
	2WS + DYC	0.0826	0.6242	0.0908	0.0524

LQC: linear quadratic control; MPC: model predictive control; 2WS: two-wheel steering; 4WS: four-wheel steering; DYC: direct yaw moment control.

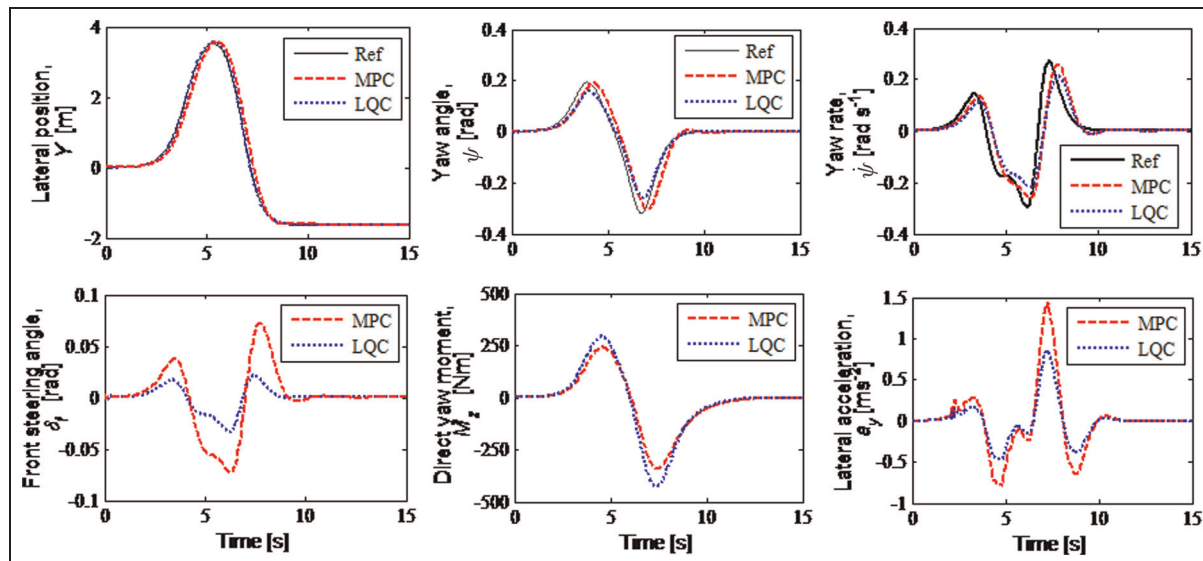
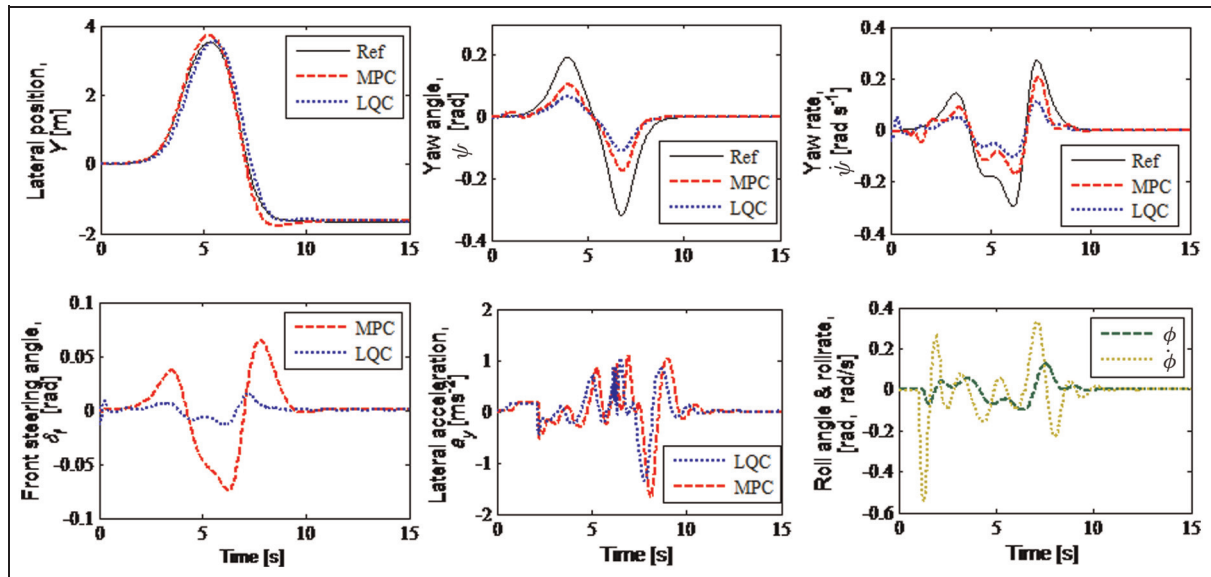
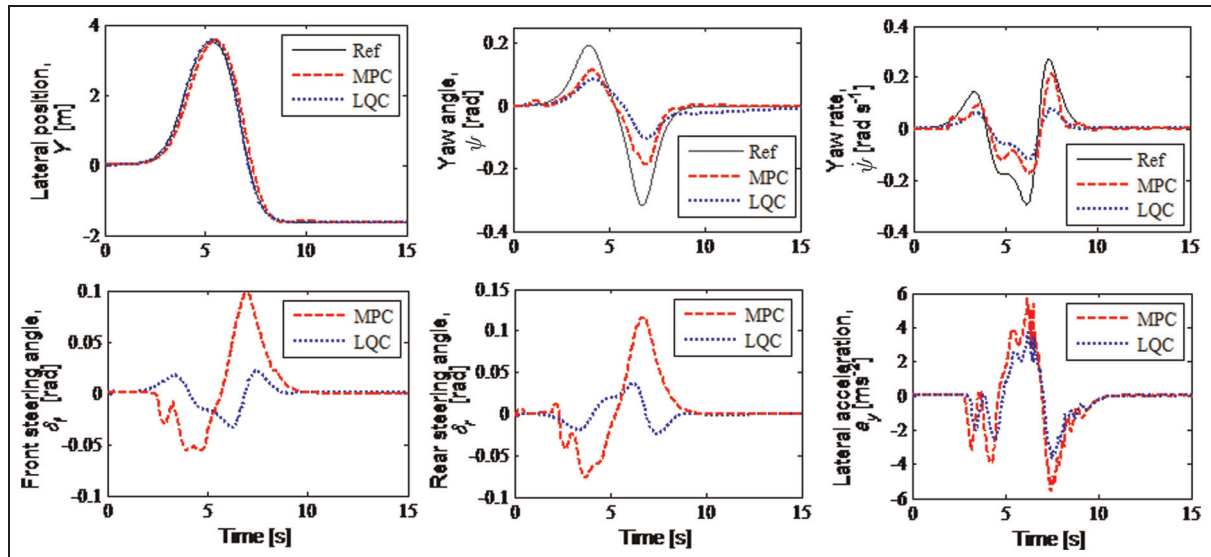


Figure 10. Vehicle manoeuvre by 2WS with DYC at 10 m/s.

Ref: reference; MPC: model predictive control; LQC: linear quadratic control.

**Figure 11.** Vehicle manoeuvre by 2WS at 25 m/s.

Ref: reference; MPC: model predictive control; LQC: linear quadratic control.

**Figure 12.** Vehicle manoeuvre by 4WS at 25 m/s with $\mu=1$.

Ref: reference; MPC: model predictive control; LQC: linear quadratic control.

similar for LQC, but it can be seen that LQC did not perform well in terms of the yaw angle and the yaw rate tracking responses. This shows that LQC is not suitable for control implementation in multi-variable systems.

Moreover, Figures 12 and 13 illustrate that, for a high forward speed of the vehicle, the manoeuvre response was much better for 4WS and for 2WS with DYC than for 2WS; the rear steering and DYC were fully utilized. We can therefore conclude that, for 4WS, the rear wheels helped the vehicle to steer by improving its handling at a high speed and decreasing the turning radius at a low speed. In 2WS vehicles, the rear set of wheels are always directed forwards and do not play an active role in controlling the steering. To illustrate our

point, the tracking-error result based on equation (45) for all the manoeuvres from Figures 11 to 13 are listed in Table 4, from which it can be seen that, of the three manoeuvre controls, 2WS with DYC gives the best performance by reducing the tracking error for the lateral position, the yaw angle and the yaw rate responses compared with those for 4WS and for 2WS alone. However, in some cases (in particular, at high speeds with neglected road friction), the lateral position is much lower under 4WS of the model predictive controller than for the other manoeuvre controls.

Next, we tested the vehicle at a forward speed of 20 m/s and taking the road friction coefficient to be that for wet earth with snow ($\mu = 0.3$), with the tuning

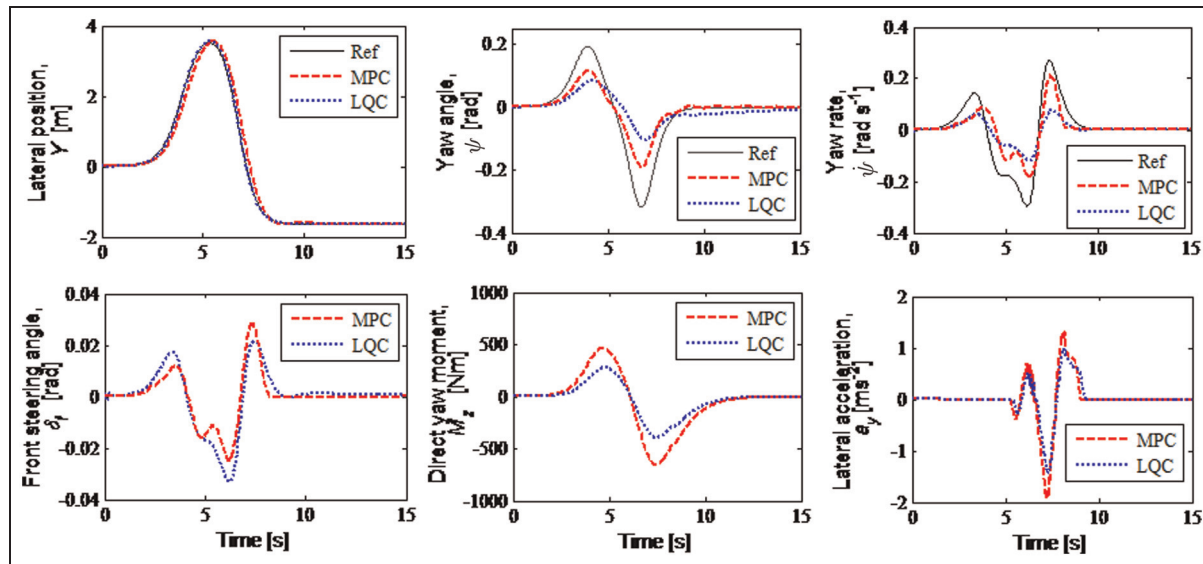


Figure 13. Vehicle manoeuvre by 2WS with DYC at 25 m/s.

Ref: reference; MPC: model predictive control; LQC: linear quadratic control.

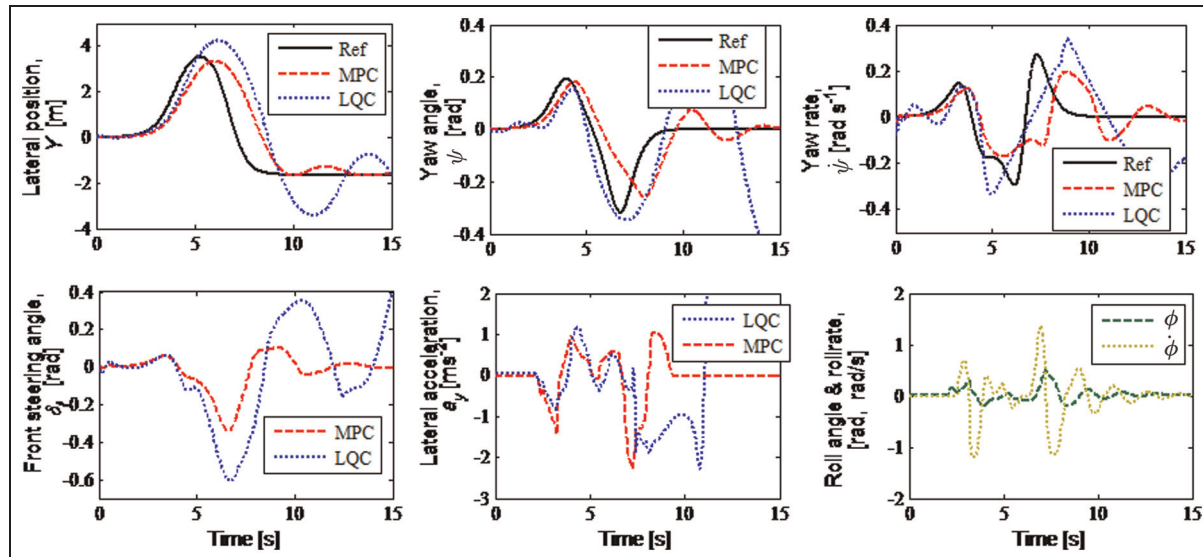


Figure 14. Vehicle manoeuvre via 2WS at 20 m/s with $\mu = 0.3$.

Ref: reference; MPC: model predictive control; LQC: linear quadratic control.

parameters for MPC and LQC as listed in Table 3. In these scenarios, we ignored the simulations under a low forward speed because we believe that the vehicle response is not really influenced at a low speed. Thus, we compare the simulation results for 2WS, 4WS and 2WS with DYC for both controllers at a middle forward speed with a low road friction coefficient, as shown in Figure 14, Figure 15 and Figure 16 respectively. These results show that at 20 m/s, and when μ varies from its values for asphalt and dry concrete to wet earth with snow, 4WS and 2WS with DYC manoeuvres give much better tracking performances than does 2WS alone. It can be noted that, for 4WS and

2WS with DYC, MPC performed much better than LQC in terms of the yaw angle and the yaw rate tracking responses. However, the MPC and LQC tracking responses for the 2WS manoeuvre were unstable, with the result that the vehicle loses control and spins away from the trajectory.

In these scenarios, we can see clearly that, for 4WS, the rear wheels helped the vehicle to steer by improving its handling at low-friction adhesion, while it is the same for 2WS with DYC, where DYC is fully utilized to stabilize the vehicle along the trajectory at a middle speed, as shown from the yaw angle and the yaw rate vehicle responses. Furthermore, the simulation results

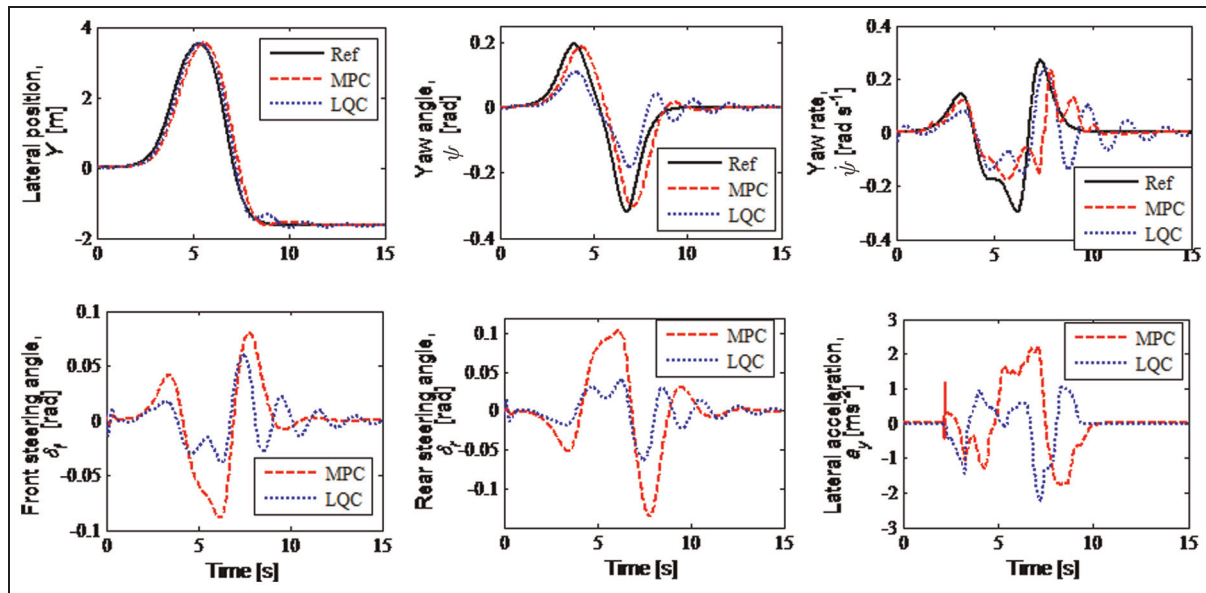


Figure 15. Vehicle manoeuvre via 4WS at 20 m/s with $\mu = 0.3$.

Ref: reference; MPC: model predictive control; LQC: linear quadratic control.

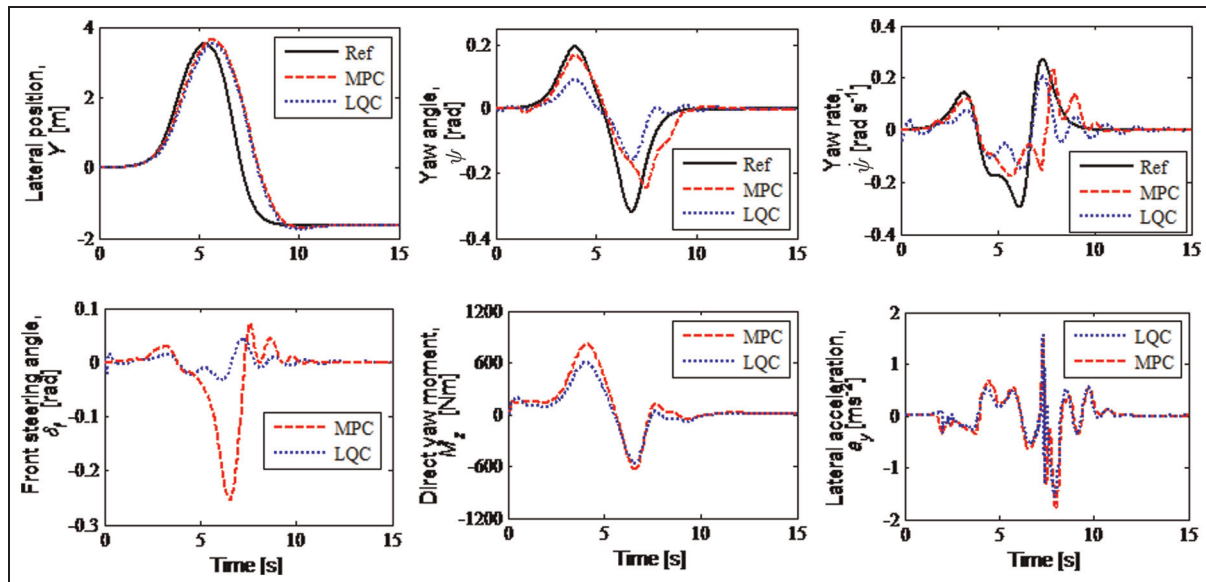


Figure 16. Vehicle manoeuvre via 2WS with DYC at 20 m/s with $\mu = 0.3$.

Ref: reference; MPC: model predictive control; LQC: linear quadratic control.

in Figures 15 and 16 also demonstrate that, for both controllers, at $\mu = 0.3$ and 20 m/s, the tracking performances for the lateral position and the yaw rate were better, but not perfect and still allowed the vehicle to track and follow the trajectory compared with Figure 14. Table 5 shows the robustness values of the controller performance and the tracking errors for all types of manoeuvre at a vehicle speed of 20 m/s with road surface friction.

Finally, we simulated the vehicle's behaviour at a high forward speed of 25 m/s with an ideal road surface friction coefficient (dry asphalt; $\mu = 1$) and at a middle forward speed of 20 m/s, taking the road surface

friction condition to be wet earth with snow ($\mu = 0.3$), in a double-lane-change scenario to minimize the tracking errors. We used MPC with an FF controller and compared the results with those from LQC with an FF controller described in the section on LQC and the section on MPC with an FF controller. Table 6 illustrates the weighting matrices for MPC and LQC with FF controller gain parameters, for each control manoeuvre. We compared the performances of both controllers for the lateral position and the yaw angle output responses to an active front steering manoeuvre alone, as shown in Figures 17 and 18. The idea for this scenario was selected because we wanted to see the

Table 5. Path-following tracking errors with road-surface friction $\mu = 0.3$.

Vehicle speed (m/s)	Manoeuvre control	LQC		MPC	
		Y (m)	ψ (rad)	Y (m)	ψ (rad)
20	2WS	0.8424	0.5654	0.5876	0.3014
	4WS	0.1048	0.0676	0.0954	0.0184
	2WS + DYC	0.1487	0.0986	0.1394	0.0268

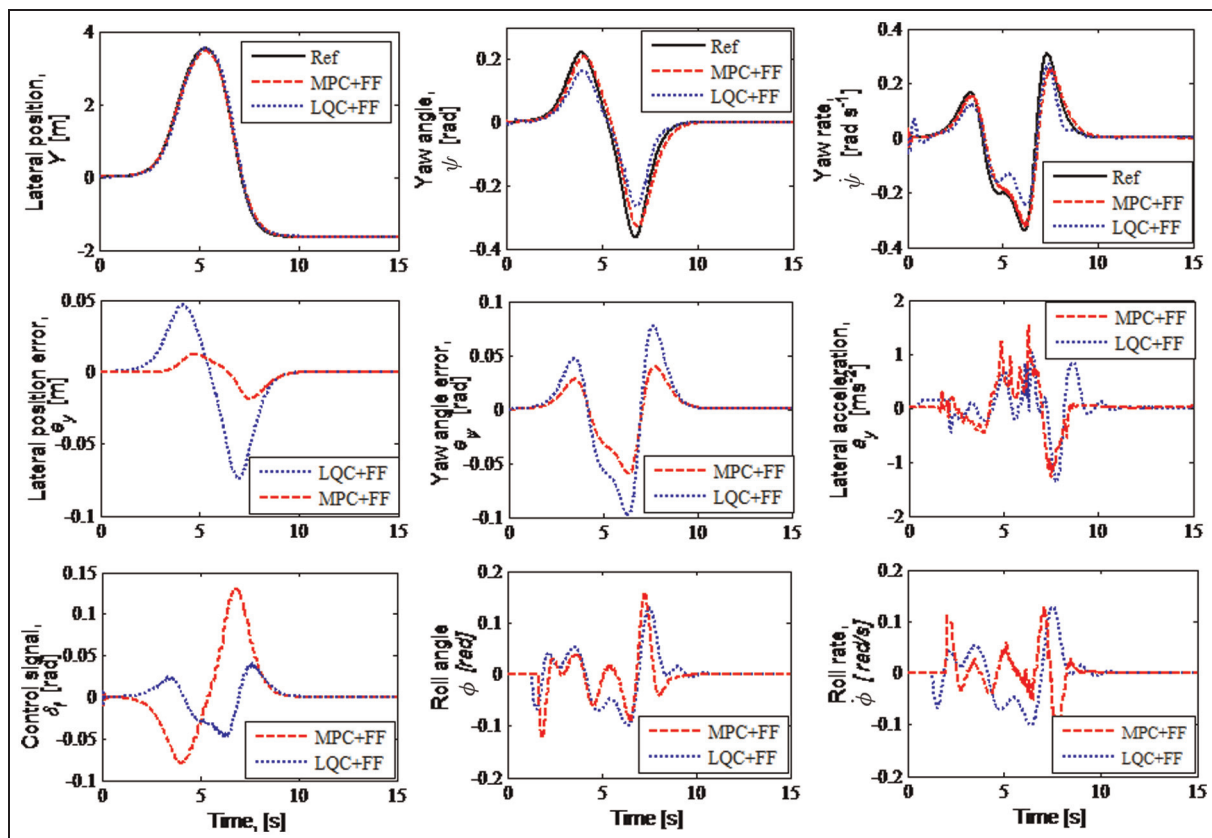
Table 6. Parameters of the weighting matrices of the controllers.

Control manoeuvres	MPC + FF	LQC + FF
2WS	$v_x = 25 \text{ m/s}, \mu = 1$	$R_1 = 0.1$ $Q_{11} = 4.25$ $Q_{22} = 1.5$ $k_{ff1} = 2.45$ $k_{ff2} = 1.25$ $R_1 = 0.1$ $Q_{11} = 3.85$ $Q_{22} = 1.25$ $k_{ff1} = 1.95$ $k_{ff2} = 0.75$ $R_{lq} = 5$ $Q_{lq1} = 18.5$ $Q_{lq2} = 3.5$ $K_f = 1.25$ $K_s = 1.45$ $R_{lq} = 5$ $Q_{lq1} = 12.5$ $Q_{lq2} = 2.8$ $K_f = 0.95$ $K_s = 1.15$
	$v_x = 20 \text{ m/s}, \mu = 0.3$	

MPC: model predictive control; LQC: linear quadratic control; FF: feedforward; 2WS: two-wheel steering.

effect of the FF controller compared with the results in Figures 11 and 14 without the FF term. From Figures 17 and 18, it can be clearly seen that, for MPC with an FF controller, the trajectory tracking responses for the lateral position and the yaw angle in 2WS were slightly better than for LQC with an FF controller. Figure 17 demonstrates that both controllers performed very well for the lateral position, but that MPC with an FF controller performed much better than LQC with an FF controller for the yaw angle and the yaw rate responses. Moreover, the lateral position and the yaw angle errors are greatly reduced by adding an FF controller to either MPC or LQC.

Furthermore, when the vehicle behaviour is simulated on a low-road-adhesion surface, as shown in Figure 18, MPC with an FF controller still behaves

**Figure 17.** Vehicle tracking errors for a manoeuvre via 2WS at 25 m/s with $\mu = 1$. Ref: reference; MPC: model predictive control; FF: feedforward; LQC: linear quadratic control.

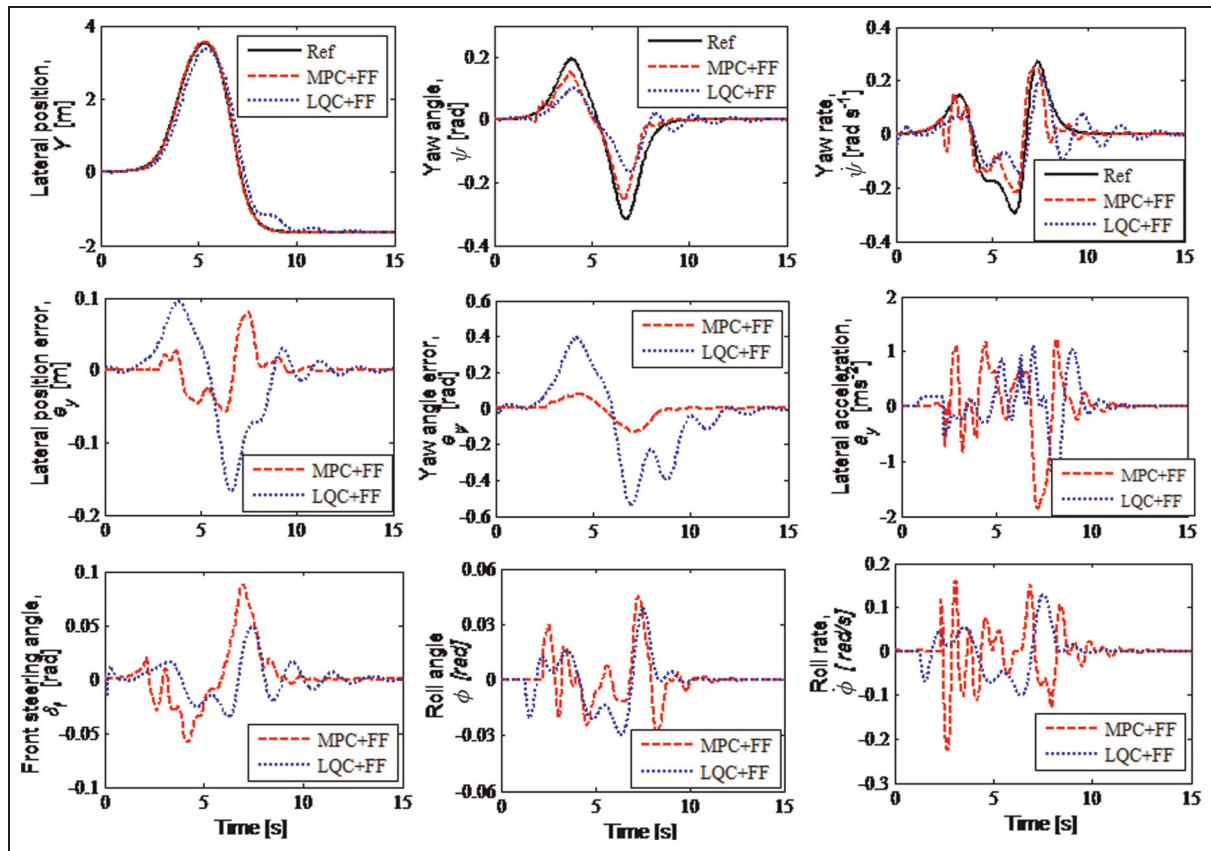


Figure 18. Vehicle tracking errors for a manoeuvre via 2WS at 20 m/s with $\mu = 0.3$.

Ref: reference; MPC: model predictive control; FF: feedforward; LQC: linear quadratic control.

better than LQC with an FF controller for both output responses. However, in this situation, it can be seen that, for the yaw angle and the yaw rate responses, the vehicle does not follow the trajectory very well. It has some vibrations or oscillations for both controllers, which causes the vehicle performances to deteriorate; from the present authors' knowledge, this arises from the tuning gain parameter of the FF controller or the initial conditions of the system. However, for a low friction coefficient, MPC with an FF controller still gives better responses than LQC with an FF controller. It can also be seen that, when an FF controller is added to MPC or LQC, the trajectory-tracking response is again much better than with MPC or LQC alone.

Last but not least, we address the issue of improving the tracking responses, by using appropriate tuning weighting matrices and prediction and control horizons for MPC and LQC. A proper adjustment of the weighting matrices should provide a better response; therefore, in this paper, we tuned the parameters using a trial-and-error procedure and then selected the best tuning weighting matrices based on the best performances.

Conclusion

This paper presented a comprehensive study of MPC and LQC of an autonomous vehicle in path-following control. The study focused on different control

manoeuvres (2WS, 4WS and 2WS with DYC) at a low forward speed, a middle forward speed and a high forward speed on various road surfaces (a high friction coefficient; dry concrete and a low friction coefficient; wet earth with snow) in a double-lane-change scenario. The controllers were designed on the basis of a simple 2DoF vehicle model with a linear tyre model, and the system was based on yaw-roll motion with a non-linear tyre model. On the basis of a known trajectory for the lateral position and the yaw angle, we evaluated the effect of roll dynamics at a low speed (10 m/s), a middle speed (20 m/s) and a high speed (25 m/s), at a high road friction ($\mu = 1$) and a low road frictions ($\mu = 0.3$), to follow the trajectory as closely as possible while maintaining the vehicle stability. Moreover, we evaluated and compared the efficiency of the front steering, the rear steering and the direct yaw moment as control inputs to the system. We also proposed MPC with an FF controller to minimize the trajectory errors for the lateral position and the yaw angle and thus to enhance the vehicle stability. We showed that, by adding an FF controller, it enhances the vehicle stability and improves the lateral position tracking.

The simulation results showed that including the roll dynamics in the linear vehicle model leads to considerable improvements in the stability and trajectory performance of the vehicle. Furthermore, the results showed that use of the rear wheels and the direct yaw

moment are beneficial in helping to steer the vehicle, improving its handling at a high speed, decreasing the turning radius at a low speed and reducing the tracking errors for the lateral position and the yaw rate responses. The simulations also proved that MPC is more useful than LQC for multi-variable systems and systems with constraints. However, we highlighted that there is a trade-off for the controllers to achieve the target for two tracking outputs with one control signal. Thus, MPC is very useful when implemented for multi-variable systems with constraints compared with LQC. Currently, we are seeking to solve the trade-off between the lateral position and the yaw rate responses to achieve better responses for both trajectories. Comparison of the performances for real non-linear models is left for further work.

Acknowledgements

The authors would like to thank Zidong Wang and Manfred Ploechl for their comments and advice. Special thanks are also extended to Ahmad Zahran Md Khudzari for his help in preparing this paper.

Funding

This work was financially supported through the Asian Human Resource Fund by the Tokyo Metropolitan Government (grant number).

Declaration of conflict of interest

The authors declare that there is no conflict of interest.

References

- Camacho EF and Bordons C. *Model predictive control*. 2nd edition. London: Springer, 2007.
- Garcia CE, Prett DM and Morari M. Model predictive control: theory and practice. *Automatica* 1989; 3(25): 335–348.
- Maciejowski JM. *Predictive control with constraints*. London: Prentice Hall, 2002.
- Bemporad A and Morari M. Robust model predictive control: a survey. In: *Robustness in identification and control*, Lecture Notes in Control and Information Sciences, Vol 245, 1999, pp. 207–226. Berlin: Springer.
- Leva A and Bascetta L. Designing the feedforward part of 2-d.o.f. industrial controllers for optimal tracking. *Control Engng Practice* 2007; 15(8): 909–921.
- Matthew OTC and Theeraphong W. Optimal LQ feed-forward tracking with preview: practical design for rigid body motion control. *Control Engng Practice* 2014; 26: 41–50.
- Zou Q. Optimal preview-based stable inversion for output tracking of nonminimum-phase systems. *Automatica* 2009; 45(1): 230–237.
- Chang S and Gordon TJ. A flexible hierarchical model-based control methodology for vehicle active safety systems. *Veh System Dynamics* 2008; 46(Suppl): 63–75.
- Kamal M, Mukai M, Murata J and Kawabe T. Ecological vehicle control on roads with up-down slopes. *IEEE Trans Intell Transpn Systems* 2011; 12(3): 783–794.
- Nagai M, Shino M and Gao F. Study on integrated control of active front steer angle and direct yaw moment. *JSAE Rev* 2002; 23(3): 309–315.
- Falcone P, Tseng HE, Borrelli F et al. MPC-based yaw and lateral stabilisation via active front steering and braking. *Veh System Dynamics* 2008; 46(1): 611–628.
- Keen SD and Cole DJ. Steering control using model predictive control and multiple internal models. In: *8th international symposium on advanced vehicle control*, Taipei, Republic of China, 20–24 August 2006, pp. 1–6. Tokyo: JSAE.
- Manfred P and Johannes E. Driver models in automobile dynamics application. *Veh System Dynamics* 2007; 45(7–8): 699–741.
- Adireddy G and Shim T. MPC based integrated chassis control to enhance vehicle handling considering roll stability. In: *ASME 2011 dynamic systems and control conference and Bath/ASME symposium on fluid power and motion control*, Arlington, Virginia, USA, 31 October–2 November 2011, Vol 2, paper DSAC2011-6159, pp. 877–884. New York: ASME.
- Anwar S. Yaw stability control of an automotive vehicle via generalized predictive algorithm. In: *2006 American control conference*, Portland, Oregon, USA, 8–10 June 2005, pp. 435–440. New York: IEEE.
- March C and Shim T. Integrated control of suspension and front steering to enhance vehicle handling. *Proc IMechE Part D: J Automobile Engineering* 2007; 221(4): 377–391.
- Tanelli M, Vecchio C, Corno M et al. Traction control for ride-by-wire sport motorcycles: a second order sliding mode approach. *IEEE Trans Ind Electron* 2009; 56(9): 3347–3356.
- Canale M, Fagiano L, Milanese M and Borodani P. Robust vehicle yaw control using active differential and internal model control techniques. In: *2006 American control conference*, Minneapolis, Minnesota, USA, 14–16 June 2006, pp. 1–6. New York: IEEE.
- Conde EC, Carbajal FB, Gonzaä lez AV and Bracamontes RC. Robust control of active vehicle suspension systems using sliding modes and differential flatness with MATLAB. In: K Perutka (ed) *MATLAB for engineers – applications in control, electrical engineering, IT and robotics*. Rijeka: InTech, 2011, ch 18.
- Wang J, Wilson DA, Xu W and Crolla DA. Integrated vehicle ride and steady-state handling control via active suspensions. *Int J Veh Des* 2006; 2(3): 306–327.
- Lee JH and Yoo WS. Predictive control of a vehicle trajectory using a coupled vector with vehicle velocity and sideslip angle. *Int J Automot Technol* 2009; 10(2): 211–217.
- Park JM, Kim DW, Yoon YS et al. Obstacles avoidance of autonomous vehicle based on model predictive control. *Proc IMechE Part D: J Automobile Engineering* 2009; 223(12): 1499–1516.
- Falcone P, Borrelli F, Asgari J et al. Predictive active steering control for autonomous vehicle systems. *IEEE Trans Control System Technol* 2007; 15(3): 566–580.
- Nam K, Oh S, Fujimoto H and Hori Y. Robust yaw stability control for electric vehicles based on active front steering control through a steer-by-wire system. *Int J Automot Technol* 2012; 13(7): 1169–1176.
- Bianchi D, Borri A, Di Benedetto MD et al. Adaptive integrated vehicle control using active front steering and

- rear torque vectoring. *Intl J Veh Autonomous Systems* 2010; 8(2–4): 85–105.
26. Ackermann J and Sienel W. Robust yaw damping of cars with front and rear wheel steering. *IEEE Trans Control Systems Technol* 1993; 1(1): 15–20.
 27. Yoshida H, Shinohara S and Nagai M. Lane change steering manoeuvre using model predictive control theory. *Veh System Dynamics* 2008; 46(Suppl): 669–681.
 28. Abe M, Ohkubo N and Kano Y. A direct yaw moment control for improving limit performance of vehicle handling – comparison and cooperation with 4WS. *Veh System Dynamics* 1996; 25(Suppl 1): 3–23.
 29. Arabi S and Behroozi M. Design of an integrated active front steering and active rear differential controller using fuzzy logic control. In: *World congress on engineering*, London, UK, 30 June–2 July 2010, Vol II, pp. 1–6. Hong Kong: International Association of Engineers.
 30. Kim W, Kim D, Yi K and Kim HJ. Development of a path-tracking control system based on model predictive control using infrastructure sensors. *Veh System Dynamics* 2012; 50(6): 1001–1023.
 31. Borrelli F, Falcone P, Keviczky L et al. MPC-based approach to active steering for autonomous vehicle systems. *Int J Veh Autonomous Systems* 2005; 3(2–4): 265–291.
 32. Chen B and Peng H. Differential-braking-based rollover prevention for sport utility vehicles with human-in-the-loop evaluations. *Veh System Dynamics* 2001; 36(4–5): 359–389.
 33. Pacejka H. *Tire and vehicle dynamics*. 3rd edition. Oxford: Elsevier, 2012.
 34. Katriniok A and Abel D. LTV-MPC approach for lateral vehicle guidance by front steering at limits of vehicle dynamics. In: *2011 50th conference on decision and control and European control conference*, Orlando, Florida, USA, 12–15 December 2011, pp. 6828–6833. New York: IEEE.
 35. Mayne DQ, Rawlings JB, Rao CV and Scokaert POM. Constrained model predictive control: stability and optimality. *Automatica* 2000; 36(6): 789–814.
 36. Groves KP, Sigthorsson DO, Serrani A et al. Reference command tracking for a linearized model of an air-breathing hypersonic vehicle. In: *AIAA guidance, navigation, and control conference and exhibit*, San Francisco, California, USA, 15–18 August 2005, paper AIAA-2005-6144, pp. 2901–2914. Reston, Virginia: AIAA.
 37. Hammar G and Ovtchinnikov V. *Structural intelligent platooning by a systematic LQR algorithm*. Master's Thesis, Royal Institute of Technology, KTH, Stockholm, Sweden, October 2010.
 38. Sharp RS and Valtetsiotis V. Optimal preview car steering control. *Veh System Dynamics* 2001; 35(Suppl): 101–117.
 39. Cole DJ, Pick AJ and Odhams AMC. Predictive and linear quadratic methods for modelling driver steering control. *Veh System Dynamics* 2006; 44(3): 259–284.
 40. MacAdam C. Application of an optimal preview control for simulation of closed-loop automobile driving. *IEEE Trans Systems, Man, Cybernetics* 1981; 11(6): 393–399.
 41. Rajamani R. *Vehicle dynamics and control*. 2nd edition. New York: Springer, 2012.
 42. Viano DC and Parenteau C. Case study of vehicle maneuvers leading to rollovers: need for a vehicle test simulating off road excursions, recovery and handling. SAE paper 2003-01-0169, 2003.

Appendix I

Notation

b_ϕ	equivalent roll damping coefficient of the suspension (N m s)
b_w	damping coefficient of the driveline (N m s)
C_f, C_r	linear approximations of the tyre stiffnesses for the front tyres and rear tyres respectively (N/rad)
e_t	tracking error
e_ψ	vehicle yaw angle error with respect to the road (deg)
e_x	longitudinal position error of the vehicle (m)
e_y	lateral position error of the centre of gravity of the vehicle with respect to the centre-line of the lane (m)
F_x, F_y	longitudinal tyre force and lateral tyre force respectively (N)
F_z	normal tyre load force (N)
g	acceleration due to gravity (m/s ²)
h	distance between the centre of gravity of the vehicle and the assumed roll axis (m)
h_{uf}, h_{ur}	distances of the front roll centre and rear roll centre respectively below the centre of gravity of the sprung mass (m)
H_p, H_c	prediction horizon and control horizon respectively
I_{xx}	inertia around the roll x axis (kg m ²)
I_{xz}	inertia product around the roll and yaw axes (kg m ²)
I_{zz}	inertia around the yaw z axis (kg m ²)
J	cost function of model predictive control and linear quadratic control
J_b	inertia of the tyres and wheels (kg m ²)
k_{ff}	feedforward gain
k_{ss}	steady-state steering angle
k_ϕ	equivalent roll stiffness coefficient of the suspension (N m)
l	vehicle wheelbase length (m)
l_f, l_r	distances of the front wheels and the rear wheels respectively from the centre of gravity (m)
m	mass of the vehicle (kg)
M_f, M_r	reaction moments at the front wheels and rear wheels respectively (N m)
M_z	total reaction moment (N m)
n	number of time periods of the r.m.s. error
Q, R	weighting matrices of model predictive control and linear quadratic control respectively
r_i	reference input
r_w	radius of the wheels (m)
R_w	radius of the circular road (m)
s	slip ratio of the tyres
t_w	track width of the vehicle (m)
T	simulation time (s)
T_b	braking torque (N m/s)

T_s	sampling time (s)	μ	friction coefficient of the track
Y	lateral position (m)	ψ	yaw angle (deg)
u	control input signal of the prediction model	$\dot{\phi}$	roll angle (deg)
v_x, v_y	longitudinal velocity and lateral velocity respectively of the vehicle (m/s)	$\dot{\psi}$	yaw rate (deg/s)
x, y, z	coordinates of the position of the vehicle in the body frame	$\dot{\phi}$	roll rate (deg/s)
α_f, α_r	front slip angle and rear slip angle respectively (deg)	ω_w	angular velocity of the tyres (m/s)
β	side-slip angle of the vehicle (deg)	$(\cdot)_f, (\cdot)_r$	variables at the front wheels and the rear wheels respectively
δ_f, δ_r	steering angles of the front wheels and the rear wheels respectively (deg)		
Δu	control rate input signal of the prediction model		
ΔM_z	change in the total reaction moment (N m)		
$\Delta\delta_f, \Delta\delta_r$	changes in the steering angles of the front wheels and the rear wheels respectively (deg/s)		

Abbreviations

DoF	degree of freedom
DYC	direct yaw moment control
FF	feedforward
LQC	linear quadratic control
MPC	model predictive control
QP	quadratic program
2WS	two-wheel steering
4WS	four-wheel steering